DAFTAR PUSTAKA

Aizawa, M., 2020. Development of bioceramics with life functions by harnessing crystallographic anisotropy and their biological evaluations. Journal of the Ceramic Society of Japan. 128(12), 997–1004. doi: 10.2109/jcersj2.20161.

Akmal, Y., Rahman, M., Muliari, M. and Batubara, A.S., 2022. Osteocranium of the sailfish (Istiophorus platypterus, Shaw & Nodder, 1792) from Malacca strait. Jurnal Perikanan Universitas Gadjah Mada. 24(2), 137-145. doi: 10.22146/jfs.73573.

Anggraini, R.M., Restianingsih, T., Deswardani, F., Fendriani, Y. and Purba, R.A.P., 2023. Characterization of hydroxyapatite from Channa striata and Scomberomorus commerson fish bone by heat treatment. JoP. 9(1), 49-54. doi: 10.22437/jop.v9i1.28727.

Anggresani, L., Perawati, S., Afandi, R. and Rahmadevi, 2022. Jelly candy hydroxyapatite from mackerel fish bone. Pharmacy and Pharmaceutical Sciences Journal. 9(3), 279-289. doi: 10.20473/jfiki.v9i32022.279-289.

Athinarayanan, J., Periasamy, V.S. and Alshatwi, A.A., 2020. Simultaneous fabrication of carbon nanodots and hydroxyapatite nanoparticles from fish scale for biomedical applications. Materials Science and Engineering C. 117, 1-12. doi: 10.1016/j.msec.2020.111313.

Barabás, R., Czikó, M., Dékány, I., Bizo, L. and Bogya, E.S., 2013. Comparative study of particle size analysis of hydroxyapatite-based nanomaterials. Chemical Papers. 67(11), 1414-1423. doi: 10.2478/s11696-013-0409-6.

Bee, S.L. and Hamid, Z.A.A., 2020. Hydroxyapatite derived from food industry bio-wastes: Syntheses, properties and its potential multifunctional applications. Ceramics International, 46(11), 17149–17175. doi: 10.1016/j.ceramint.2020.04.103.

Castro, M.A.M. et al., 2022. Synthesis of hydroxyapatite by hydrothermal and microwave irradiation methods from biogenic calcium source varying pH and synthesis time. Boletin de La Sociedad Española de Cerámica y Vidrio, 61(1), 35-41. doi: 10.1016/j.bsecv.2020.06.003.

Charlena, Suparto, I.H. and Laia, D.P.O., 2023. Synthesis and characterization of hydroxyapatite from polymesoda placans shell using wet precipitation method. Jurnal Bios Logos. 13(1), 85-96. doi: 10.35799/jlb.v13i1.47454.

DileepKumar, V.G. et al., 2022. A review on the synthesis and properties of hydroxyapatite for biomedical applications. Journal of Biomaterials Science, Polymer Edition. 33(2), 229-261. doi: 10.1080/09205063.2021.1980985.

Fatimah, S., Ragadhita, R., Al Husaeni, D. F. and Nandiyanto, A.B.D., 2022. How to calculate crystallite size from x-ray diffraction (XRD) using Scherrer method. Asean Journal of Science and Engineering. 2(1), 65-76. doi: 10.17509/ajse.v2i1.37647.

Ferrette, B.L.S. et al., 2021. Global phylogeography of sailfish: deep evolutionary

lineages with implications for fisheries management. Hydrobiologia. 848(17), 3883-3904. doi: 10.1007/s10750-021-04587-w.

Filip, D.G., Surdu, V.A., Paduraru, A.V. and Andronescu, E., 2022. Current development in biomaterials—hydroxyapatite and bioglass for applications in biomedical field: A review. Journal of Functional Biomaterials. 13(4), 1-21. doi: 10.3390/jfb13040248.

Hadiwinata, B. et al., 2023. Pengaruh suhu sintering pada sintesis hidroksiapatit dari tepung CaO cangkang rajungan (Portunus sp.). Marinade. 6(2), 37-46. Diakses dari: http://ojs.umrah.ac.id/index.php/marinade.

Hamzah, M.S.D. et al., 2023. Diet composition of Indo-Pacific sailfish (Istiophorus platypterus) by-catch in the East Coast of Peninsular Malaysia. Journal of Fisheries and Environment. 47(3), 40-49. doi: 10.1016/S0165-7836(01)00344-7.

Haris, A., Fadli, A. dan Yenti, S.R., 2016. Sintesis hidroksiapatit dari limbah tulang sapi menggunakan metode presipitasi dengan variasi rasio Ca/P dan konsentrasi H_3PO_4. JOM Fteknik. 3(2), 1-10. Diakses dari: https://jom.unri.ac.id/index.php/JOMFTEKNIK/article/view/11510.

Herliansyah, M.K., Hamdi, M., Ektessabi, A.I., Wildan, M.W. and Toque, J.A., 2009. The influence of sintering temperature on the properties of compacted bovine hydroxyapatite. Materials Science and Engineering C. 29(5), 1674-1680. doi: 10.1016/j.msec.2009.01.007.

Hussin, M.S.F., Abdullah, H.Z., Idris, M.I. and Wahap, M.A.A., 2022. Extraction of natural hydroxyapatite for biomedical applications—A review. Heliyon. 8(8), 1-11. doi: 10.1016/j.heliyon.2022.e10356.

Ibrahim, M., Labaki, M., Giraudon, J.M. and Lamonier, J.F., 2020. Hydroxyapatite, a multifunctional material for air, water and soil pollution control: A review. Journal of Hazardous Materials. 383. doi: 10.1016/j.jhazmat.2019.121139.

John, K.P., Annapurna, Y., Krishna, P. and Sreeramulu, K., 2017. Seasonal variation of proximate composition of Istiophorus platypterus from Visakhapatnam fishing harbor, East Coast of India. International Journal of Bioassays. 6(10), 5530-5534. doi: 10.21746/ijbio.2017.6.10.4.

Kumar, K.C.V. et al., 2021. Spectral characterization of hydroxyapatite extracted from Black Sumatra and Fighting cock bone samples: A comparative analysis. Saudi Journal of Biological Sciences. 28(1), 840-846. doi: 10.1016/j.sjbs.2020.11.020.

Masruroh, Manggara, A.B., Papilaka, T. dan Triandi, R., 2013. Penentuan ukuran Kristal (crytallite size) lapisan tipis PZT melalui pendekatan persamaan Debye Scherrer. Erudio Journal of Educational Innovation. 1(2), 24-29. doi: 10.18551/erudio.1-2.4.

Megawati, M., Patty, D.J. and Yusuf, Y., 2023. Synthesis and characterization of carbonate hydroxyapatite from Pinctada maxima shell with short aging time for bone biomaterial candidate. Engineering Chemistry. 3, 13-18. doi: 10.4028/p-08k84g.

Muarif, M.F., Yusuf, Y. and Agipa, A.I., 2024. FTIR, XRD, and SEM-EDX characterization of synthesized B-type carbonated hydroxyapatite (CHAp) based on crab shells. Journal of Energy, Material, and Instrumentation Technology. 5(1), 35-42. doi: 10.23960/jemit.v5i1.241.

Nikfallah, A., Mohammadi, A., Ahmadakhondi, M. and Ansari, M., 2023. Synthesis and physicochemical characterization of mesoporous hydroxyapatite and its application in toothpaste formulation. Heliyon. 9(10), 1-13. doi: 10.1016/j.heliyon.2023.e20924.

Ochoa, S.L., Lara, W.O. and Beltrán, C.E.G., 2021. Hydroxyapatite nanoparticles in drug delivery: Physicochemistry and applications. Pharmaceutics. 13(10), 1-24. doi: 10.3390/pharmaceutics13101642.

Perera, E.C.J., 2013. Study of radioactivity levels and elemental concentration in selected fish samples. M.Sc. thesis, University of Colombo.

Prekajski, M. et al., 2016. Ouzo effect-New simple nanoemulsion method for synthesis of strontium hydroxyapatite nanospheres. Journal of the European Ceramic Society. 36(5), 1293-1298. doi: 10.1016/j.jeurceramsoc.2015.11.045.

Pu'ad, N.A.S.M., Haq, R.H.A., Noh, H.M., Abdullah, H. Z., Idris, M. I. and Lee, T.C., 2019. Synthesis method of hydroxyapatite: A review. Materials Today: Proceedings. 29(1), 233-239. doi: 10.1016/j.matpr.2020.05.536.

Rahayu, S., Kurniawidi, D.W. dan Gani, A., 2018. Pemanfaatan limbah cangkang kerang darah (Pinctada maxima) sebagai sumber hidroksiapatit. Jurnal Pendidikan Fisika Dan Teknologi. 4(2), 226-231. doi: 10.29303/jpft.v4i2.839.

Rahmaniah, 2019. Sintesis dan karakterisasi hidroksiapatit dari cangkang kerang dara (Anadara granosa) sebagai bahan baku semen tambal gigi. Jurnal Teknosains. 13(1), 27-32. doi: 10.24252/teknosains.v13i1.7832.

Rey, C., Combes, C., Drouet, C. and Grossin, D., 2011. Bioactive ceramics: Physical chemistry. In: Ducheyne, P., Healy, K., Hutmacher, D., Grainger, D.E. and Kickpatrick, J. (ed.). Comprehensive Biomaterials. pp. 187-221. Elsevier Ltd. doi: 10.1016/b978-0-08-055294-1.00178-1.

Riyanto, B. and Maddu, A., 2013. Material of hydroxyapatite-based bioceramics from tuna fishbone. JPHPI. 16(2), 119-132. doi: 10.17844/jphpi.v16i2.8046.

Sirait, M., Sinulingga, K., Siregar, N. and Siregar, R.S.D., 2020. Synthesis of hydroxyapatite from limestone by using precipitation method. Journal of Physics: Conf. Series. 1462(1), 1-8. doi: 10.1088/1742-6596/1462/1/012058.

Surya, P., Nithin, A., Sundaramanickam, A. and Sathish, M., 2021. Synthesis and characterization of nano-hydroxyapatite from Sardinella longiceps fish bone and its effects on human osteoblast bone cells. Journal of the Mechanical Behavior of Biomedical Materials. 119, 1-9. doi: 10.1016/j.jmbbm.2021.104501.

Szterner, P. and Biernat, M., 2022. The synthesis of hydroxyapatite by hydrothermal process with calcium lactate pentahydrate: The effect of reagent concentrations, pH, temperature, and pressure. Bioinorganic Chemistry and Applications. 2022(1), 1-13. doi: 10.1155/2022/3481677.

Taji, L.S., Wiyono, D.E., Karisma, A.D., Surono, A. and Ningrum, E.O., 2022. Hydroxyapatite based material: Natural resources, synthesis methods, 3D print filament fabrication, and filament filler. The Journal of Engineering. 8(1), 26-35. doi: 10.12962/j23378557.v8i1.a12830.

Trung, T.S. et al., 2022. Valorization of fish and shrimp wastes to nano-hydroxyapatite/chitosan biocomposite for wastewater treatment. Journal of Science: Advanced Materials and Devices. 7(4), 1-9. doi: 10.1016/j.jsamd.2022.100485.

Wardani, N.S., Fadli, A. and Irdoni, 2015. Sintesis hidroksiapatit dari cangkang telur dengan metode presipitasi. JOM Fteknik. 2(1), 1-6. Diakses dari: https://jom.unri.ac.id/index.php/JOMFTEKNIK/article/view/6297.

LAMPIRAN 1

Prosedur Kerja

1. Preparasi tulang ikan layar

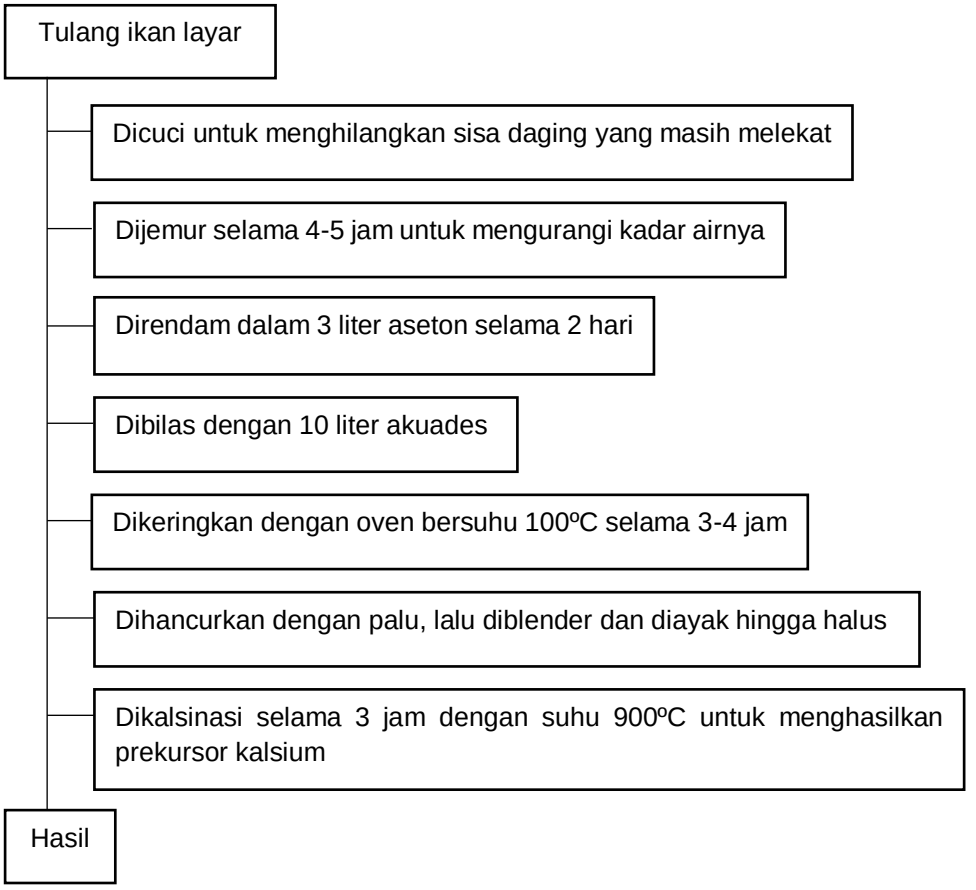

2. Sintesis HAp

Larutan 1 (Prekursor Kalsium)

Tulang ikan layar yang telah dikalsinasi sebagai prekursor kalsium

- Disiapkan prekursor kalsium sebanyak 5 gr untuk sampel A; 5,6 gr untuk sampel B; dan 6,2 gr untuk sampel C.
- Masing-masing dilarutkan ke dalam 100 ml akuades menggunakan pengaduk magnetik berkecepatan 300 rpm dengan suhu 50ºC selama 15 menit.

Hasil

Larutan 2 ($(NH_4)_2HPO_4$)

$(NH_4)_2HPO_4$

- Disiapkan $(NH_4)_2HPO_4$ sebanyak 11,9 gr untuk sampel A; 7,9 gr untuk sampel B, dan 7,3 gr untuk sampel C.
- Masing-masing dilarutkan ke dalam 100 ml akuades menggunakan pengaduk magnetik berkecepatan 300 rpm dengan suhu 50ºC selama 10 menit.

Hasil

Larutan 3 (NaOH)

NaOH

- Disiapkan 4 gr NaOH
- Dilarutkan ke dalam 100 ml akuades menggunakan pengaduk magnetik berkecepatan 300 rpm dengan suhu 50ºC selama 10 menit.

Hasil

Pembuatan Sampel A, B, dan C

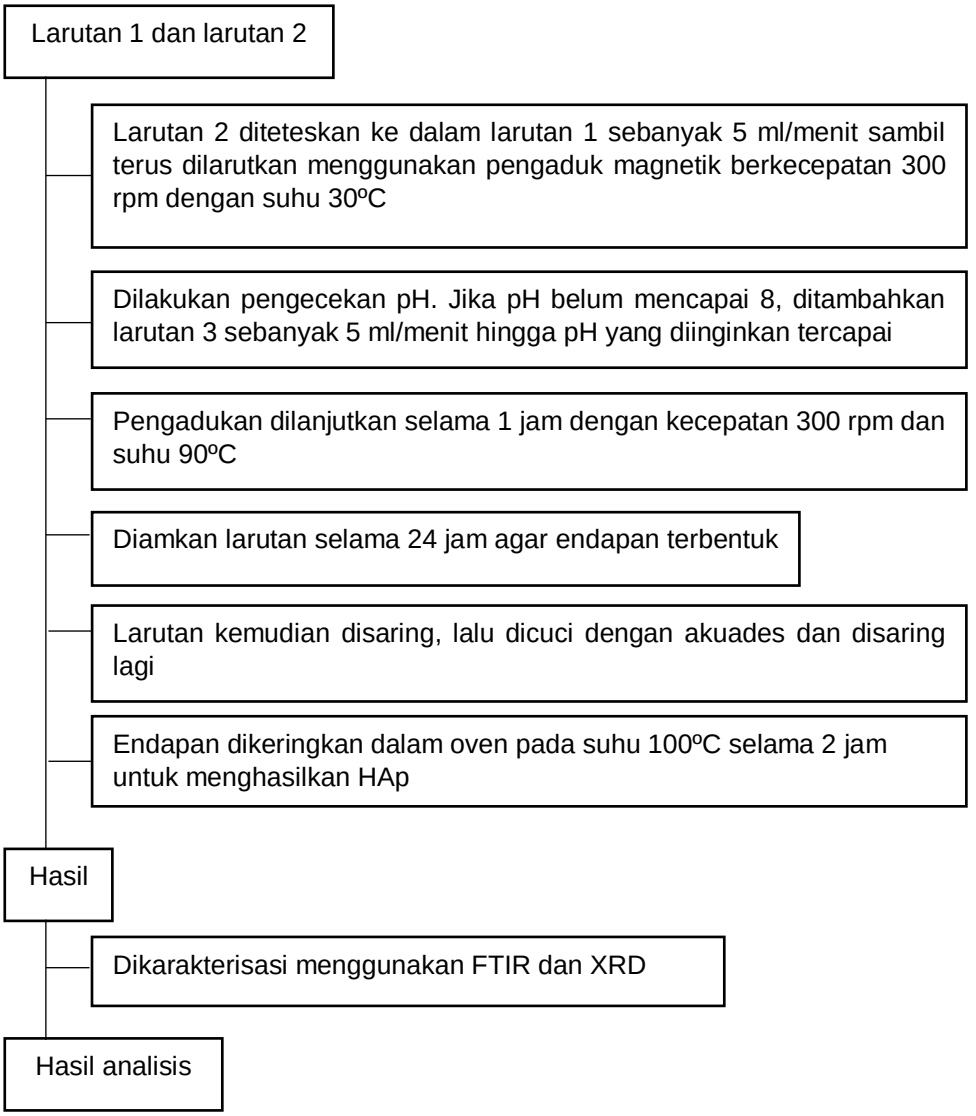

LAMPIRAN 2

Dokumentasi Kerja

Ikan layar

Sudah dicuci dan dijemur

Direndam aseton

Sudah dibilas dengan akuades

Pengeringan dengan oven

Hasil oven

Setelah di palu

Dihaluskan dengan blender

Hasil blender

Pengayakan 200 *mesh*

Hasil ayakan

Kalsinasi menggunakan *furnace*

Hasil kalsinasi

5 gr prekursor kalsium

5,6 gr prekursor kalsium

6,2 gr prekursor kalsium

11,9 gr $(NH_4)_2HPO_4$

7,9 gr $(NH_4)_2HPO_4$

7,3 gr $(NH_4)_2HPO_4$

4 gr NaOH

Larutan 1

Larutan 2

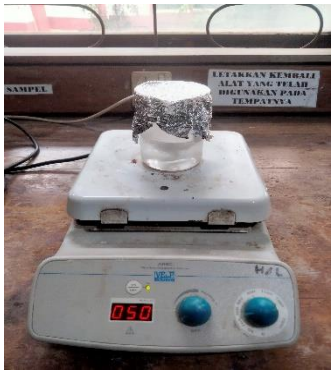

Larutan 3

Larutan 2 diteteskan ke larutan 1

pH awal

pH akhir

Larutan didiamkan selama 24 jam

Endapan terbentuk

Endapan dicuci dan disaring

Endapan sebelum dioven

Endapan setelah dioven dan jadi HAp

LAMPIRAN 3

1. Perhitungan massa $(NH_4)_2HPO_4$ untuk pembuatan larutan $(NH_4)_2HPO_4$ dengan 100 ml akuades. (Mr $(NH_4)_2HPO_4$=132,056 gr/mol)

Massa Molar $(NH_4)_2HPO_4$: N=14,007 g/mol, H=1,008 g/mol, P=30,974 g/mol, O=15,999 g/mol.

$Mr=(2\times NH_4)+HPO_4$

$Mr=(2\times(14,007+(4\times1,008))+(1,008+30,974+(4\times15,999)))$

Mr=36,078+95,978=13,056 g/mol

Sampel A (0,9 M)

$M=\frac{m}{Mr}\times\frac{1000}{V}$

$0,9=\frac{m}{132,056}\times\frac{1000}{100}$

1000 (m)=11885,04

m=11,88≈11,9 gr

Sampel B (0,6 M)

$M=\frac{m}{Mr}\times\frac{1000}{V}$

$0,6=\frac{m}{132,056}\times\frac{1000}{100}$

1000 (m)=7923,36

m=7,92≈7,9 gr

Sampel C (0,55 M)

$M=\frac{m}{Mr}\times\frac{1000}{V}$

$0,55=\frac{m}{132,056}\times\frac{1000}{100}$

1000 (m)=7263,08

m=7,26≈7,3 gr

2. Perhitungan massa NaOH untuk pembuatan larutan NaOH 1 M dengan 100 ml akuades. (Mr NaOH=40 gr/mol)

Massa Molar NaOH: Na=22,990 g/mol, O=15,999 g/mol, H=1,008 g/mol.

Mr=Na+O+H

Mr=(22,990+15,999+1,008)

Mr=39,997 g/mol

Massa NaOH:

$M=\frac{m}{Mr}\times\frac{1000}{V}$

$1=\frac{m}{39,997}\times\frac{1000}{100}$

1000 (m)=4000,0

m=4,0 gr

LAMPIRAN 4

Anasis Fase XRD menggunakan Profex 5.2.9
Sampel A

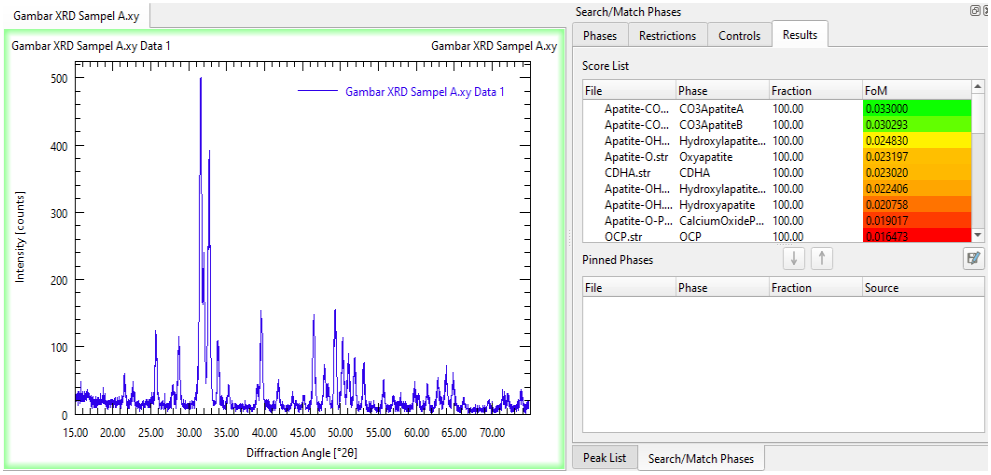

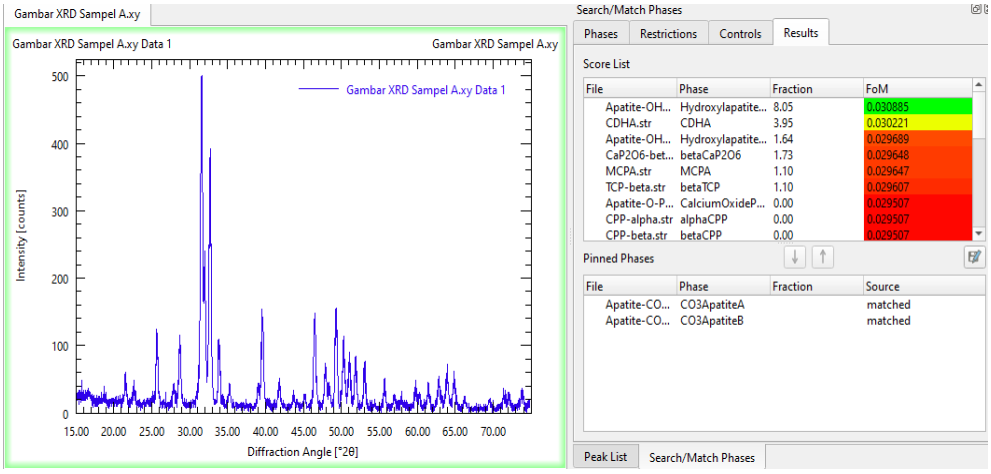

File	Phase	Fraction	FoM
DCPA.str	DCPA	0.55	0.031675
CaP2O6-bet...	betaCaP2O6	1.05	0.031651
Apatite-O-P...	CalciumOxideP...	0.00	0.031626
CDHA.str	CDHA	0.00	0.031626
Ca4P6O19.str	Ca4P6O19	0.00	0.031626
CaP4O11.str	CaP4O11	0.00	0.031626
MCPM.str	MCPM	0.00	0.031626
OCP.str	OCP	0.00	0.031626
P2O5-o.str	P2O5ortho	0.00	0.031626

Sampel B

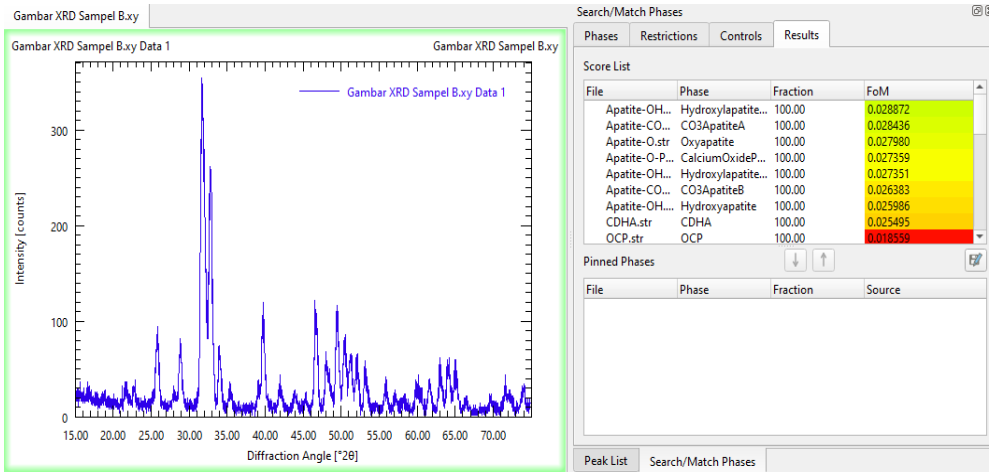

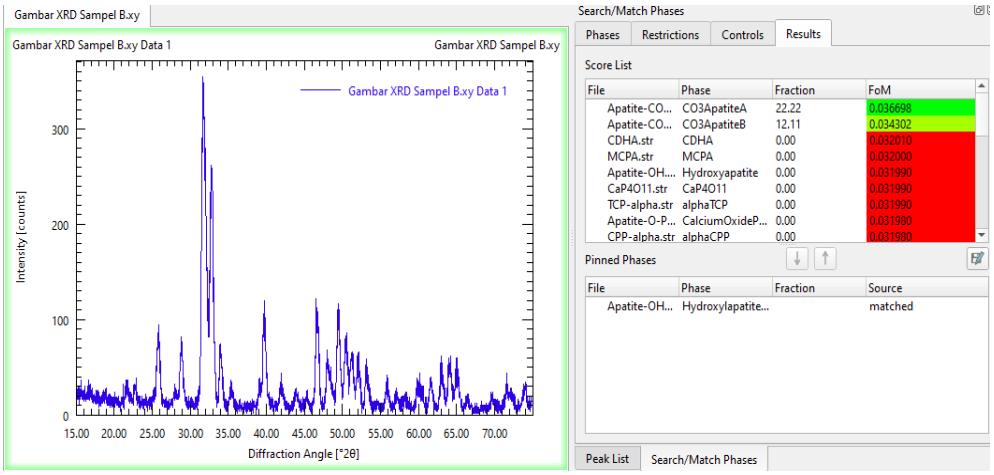

File	Phase	Fraction	FoM
OCP.str	OCP	0.00	0.035051
CDHA.str	CDHA	0.00	0.035039
Apatite-O-P...	CalciumOxideP...	0.00	0.035014
CPP-alpha.str	alphaCPP	0.00	0.035002
CPP-beta.str	betaCPP	0.00	0.035002
Ca2P6O17.str	Ca2P6O17	0.00	0.035002
P2O5-o.str	P2O5ortho	0.00	0.035002
P2O5-r.str	P2O5rhombo	0.00	0.035002
TCP-alpha.str	alphaTCP	0.00	0.035002

Sampel C

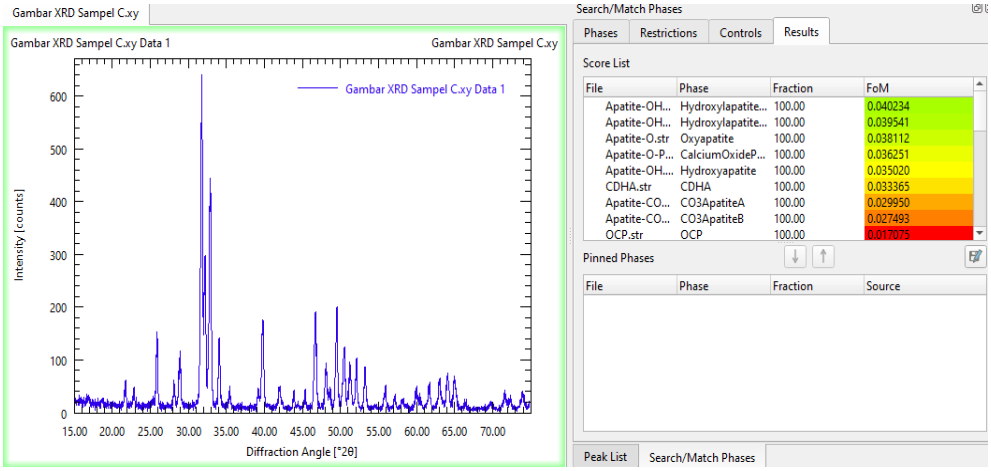

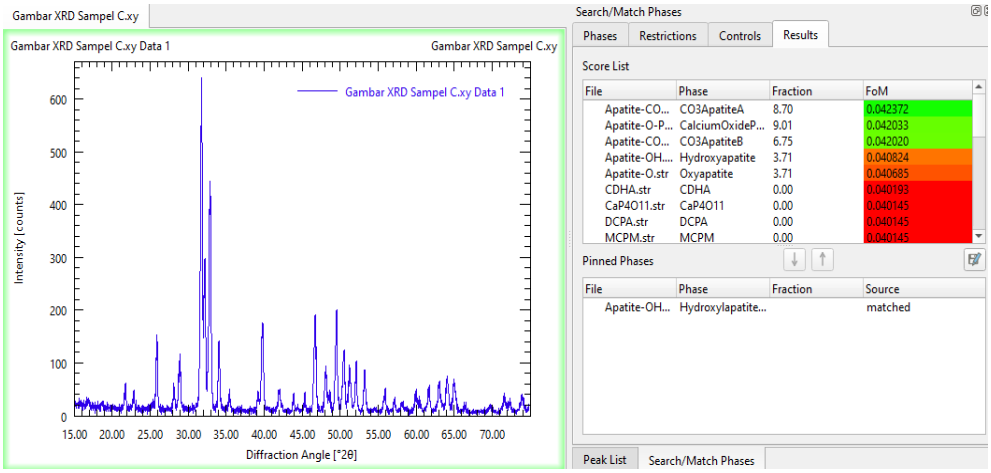

File	Phase	Fraction	FoM
DCPA.str	DCPA	0.00	0.041701
MCPM.str	MCPM	0.00	0.041701
OCP.str	OCP	0.00	0.041701
P2O5-o.str	P2O5ortho	0.00	0.041701
TCP-beta.str	betaTCP	0.00	0.041701
TetCP.str	Tetracalciumph...	0.00	0.041701
TCP-alpha.str	alphaTCP	0.00	0.041563
P2O5-o2.str	P2O5ortho2	0.00	0.041511
CaP2O6-alp...	alphaCaP2O6	0.61	0.041485

LAMPIRAN 5

Perhitungan Ukuran Kristal menggunakan Excel

Sampel	Sudut Difraksi (2θ)	θ (derajat)	cos θ	FWHM (derajat)	Ukuran Kristal (nm)	Rata-rata Ukuran Kristal (nm)	Rata-rata FWHM (derajat)
A	31,56	15,78	0,96	0,34	25,36	25,45	0,34
	31,96	15,98	0,96	0,36	23,98		
	32,69	16,34	0,96	0,32	27,02		
B	31,80	15,90	0,96	0,71	12,15	15,13	0,59
	32,81	16,41	0,96	0,57	15,18		
	46,65	23,32	0,92	0,50	18,07		
C	31,74	15,87	0,96	0,29	29,74	28,94	0,30
	32,14	16,07	0,96	0,33	26,17		
	32,87	16,44	0,96	0,28	30,90		

LAMPIRAN 6

Hasil Karakterisasi FTIR
Sampel A

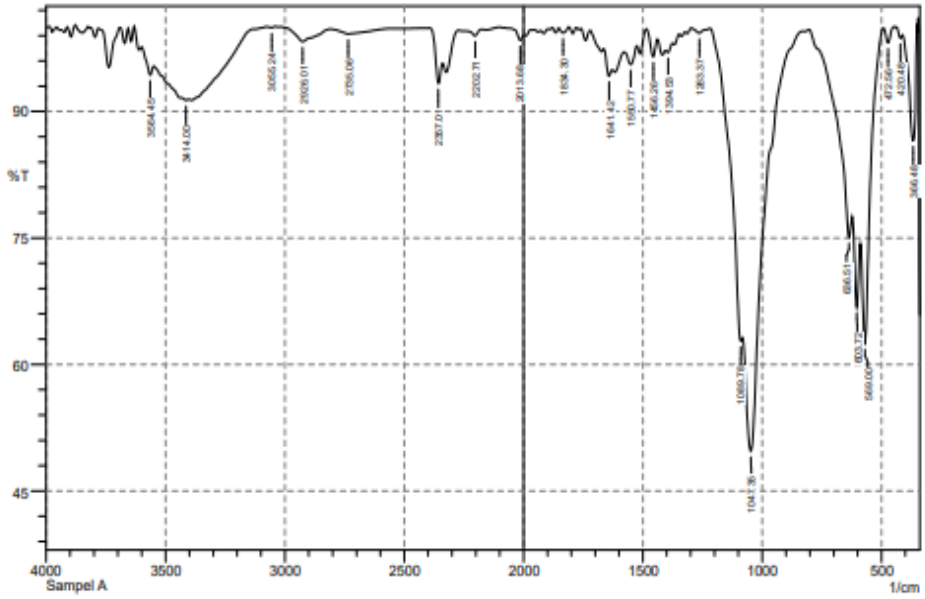

No.	Peak	Intensity	Corr. Intensity	Base (H)	Base (L)	Area	Corr. Area
1	366.48	86.561	12.748	410.84	352.97	1.926	1.731
2	420.48	98.707	0.68	437.84	410.84	0.094	0.038
3	472.56	98.134	1.822	491.85	445.56	0.165	0.159
4	569	62.475	17.041	588.29	493.78	7.989	2.421
5	603.72	66.799	8.691	621.08	590.22	4.605	0.852
6	636.51	75.061	4.148	802.39	623.01	8.179	0.36
7	1047.35	49.72	18.579	1082.07	837.11	25.239	5.5
8	1089.78	62.788	1.95	1217.08	1083.99	9.782	0.156
9	1263.37	99.301	0.578	1296.16	1217.08	0.132	0.089
10	1394.53	96.998	0.512	1404.18	1375.25	0.33	0.031
11	1456.26	96.519	2.504	1485.19	1438.9	0.408	0.241
12	1550.77	95.589	1.83	1577.77	1525.69	0.82	0.225
13	1641.42	94.205	1.64	1664.57	1627.92	0.756	0.133
14	1834.3	99.321	0.621	1851.66	1811.16	0.074	0.065
15	2013.68	98.452	0.807	2056.12	1998.25	0.194	0.055
16	2202.71	98.978	0.686	2247.07	2175.7	0.189	0.077
17	2357.01	93.342	3.723	2393.66	2339.65	0.825	0.301
18	2735.06	99.194	0.604	2812.21	2559.54	0.523	0.315
19	2926.01	98.293	1.63	3016.67	2812.21	0.727	0.646
20	3055.24	99.947	0.119	3078.39	3041.74	0	0.01
21	3414	91.344	0.152	3431.36	3404.36	1.051	0.011
22	3564.45	94.34	1.723	3599.17	3549.02	0.974	0.187

Sampel B

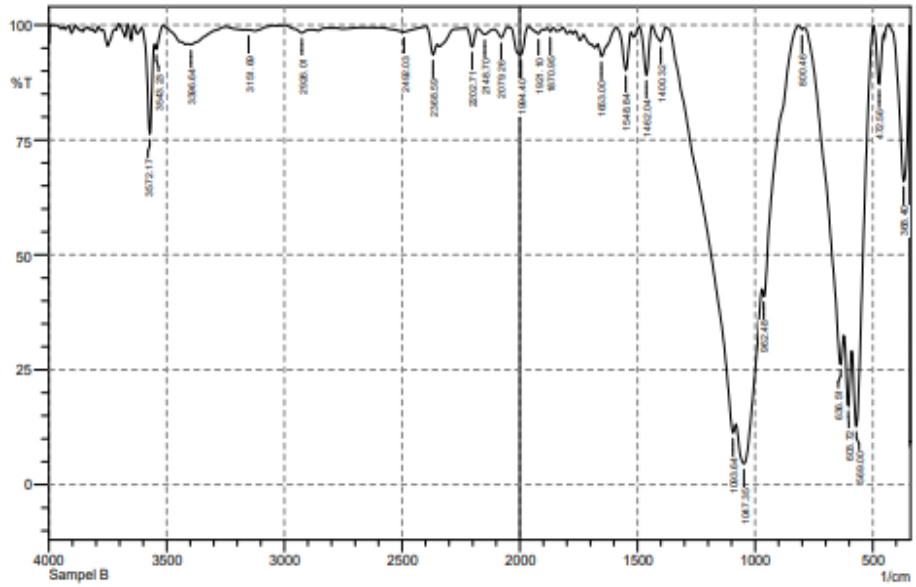

No.	Peak	Intensity	Corr. Intensity	Base (H)	Base (L)	Area	Corr. Area
1	368.4	66.063	29.809	432.05	345.26	6.73	5.624
2	472.56	87.21	11.648	495.71	453.27	1.292	1.087
3	569	12.723	31.368	588.29	497.63	34.279	11.636
4	603.72	17.268	13.154	621.08	590.22	19.603	3.68
5	636.51	26.243	11.526	790.81	623.01	35.863	2.546
6	800.46	98.994	0.502	813.96	790.81	0.064	0.017
7	962.48	41.012	4.294	970.19	815.89	20.46	0.433
8	1047.35	4.571	17.318	1080.14	972.12	96.378	28.844
9	1093.64	11.302	5.33	1363.67	1082.07	84.02	1.348
10	1400.32	96.461	3.11	1436.97	1379.1	0.524	0.422
11	1462.04	89.139	10.549	1492.9	1438.9	1.218	1.144
12	1548.84	90.173	8.604	1589.34	1527.62	1.293	1.007
13	1653	93.236	3.183	1666.5	1591.27	1.314	0.538
14	1870.95	98.58	0.742	1884.45	1857.45	0.116	0.036
15	1921.1	98.136	1.106	1961.61	1903.74	0.306	0.144
16	1994.4	93.655	5.95	2046.47	1963.53	1.287	1.141
17	2079.26	97.308	2.012	2110.12	2048.4	0.419	0.236
18	2148.7	97.965	1.187	2177.63	2110.12	0.423	0.17
19	2202.71	95.266	3.988	2227.78	2177.63	0.527	0.364
20	2368.59	93.577	3.676	2397.52	2351.23	0.79	0.327
21	2492.03	98.472	1.104	2600.04	2397.52	0.807	0.425
22	2926.01	98.293	1.029	2999.31	2887.44	0.46	0.204
23	3151.69	98.934	0.009	3163.26	3147.83	0.071	0
24	3396.64	95.737	0.464	3410.15	3251.98	1.609	0.106
25	3543.23	94.736	1.955	3550.95	3516.23	0.444	0.113
26	3572.17	76.353	20.678	3604.96	3552.88	2.668	2.079

Sampel C

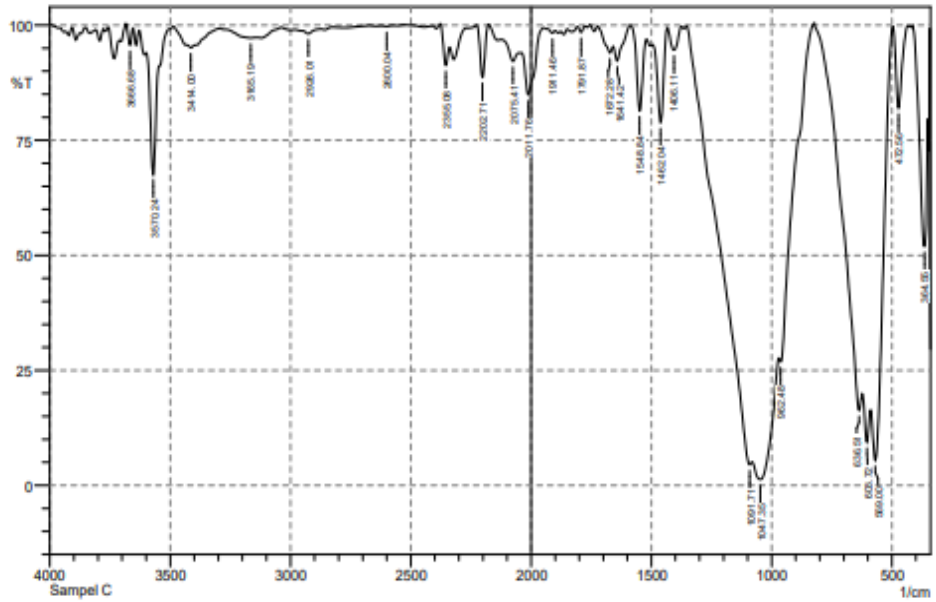

No.	Peak	Intensity	Corr. Intensity	Base (H)	Base (L)	Area	Corr. Area
1	364.55	51.993	32.565	412.77	349.12	9.249	5.984
2	472.56	82.054	17.724	495.71	432.05	2.296	2.242
3	569	5.47	28.587	588.29	497.63	47.932	15.224
4	603.72	9.403	8.283	621.08	590.22	27.306	4.106
5	636.51	16.336	8.959	821.68	623.01	51.453	2.2
6	962.48	26.914	3.556	968.27	823.6	27.963	0.462
7	1047.35	1.301	10.5	1080.14	970.19	139.587	38.539
8	1091.71	4.538	3.935	1352.1	1082.07	110.304	1.238
9	1406.11	94.656	4.929	1433.11	1375.25	0.824	0.722
10	1462.04	78.847	18.816	1492.9	1435.04	3.036	2.422
11	1548.84	81.453	16.737	1587.42	1521.84	2.515	2.059
12	1641.42	92.258	4.277	1658.78	1589.34	1.299	0.608
13	1672.28	94.007	2.135	1722.43	1660.71	1.002	0.31
14	1791.87	98.472	1.253	1807.3	1776.44	0.119	0.082
15	1911.46	98.316	0.613	1930.74	1899.88	0.178	0.041
16	2011.76	84.881	10.851	2040.69	1950.03	3.4	2.096
17	2075.41	92.192	2.708	2123.63	2052.26	1.779	0.324
18	2202.71	88.724	11.358	2225.85	2177.63	1.112	1.131
19	2355.08	91.273	6.081	2378.23	2337.72	0.912	0.5
20	2600.04	99.756	0.171	2623.19	2574.97	0.031	0.016
21	2926.01	98.141	0.778	2953.02	2873.94	0.444	0.091
22	3165.19	97.223	0.462	3294.42	3138.18	1.329	0.188
23	3414	95.149	0.976	3429.43	3296.35	1.679	0.253
24	3570.24	67.685	27.866	3599.17	3504.66	5.582	4.154
25	3666.68	95.672	4.066	3684.04	3655.11	0.283	0.263

LAMPIRAN 7

Hasil Karakterisasi XRD
Sampel A

Strongest 3 peaks

no. peak no.	2Theta (deg)	d (A)	I/I1	FWHM (deg)	Intensity (Counts)	Integrated Int (Counts)
1 7	31.5652	2.83211	100	0.33620	320	5165
2 9	32.6866	2.73746	77	0.31530	245	3920
3 8	31.9600	2.79802	42	0.35700	135	2508

Peak Data List

peak no.	2Theta (deg)	d (A)	I/I1	FWHM (deg)	Intensity (Counts)	Integrated Int (Counts)
1	21.5500	4.12029	7	0.32000	22	385
2	22.6666	3.91978	5	0.29330	15	246
3	25.6848	3.46560	22	0.29540	69	1202
4	27.9100	3.19415	5	0.30000	17	306
5	28.7080	3.10715	18	0.28000	59	935
6	31.0000	2.88245	3	0.20000	11	234
7	31.5652	2.83211	100	0.33620	320	5165
8	31.9600	2.79802	42	0.35700	135	2508
9	32.6866	2.73746	77	0.31530	245	3920
10	33.0200	2.71058	5	0.18000	15	303
11	33.8638	2.64494	19	0.29900	60	946
12	35.2400	2.54474	6	0.32000	18	347
13	39.0200	2.30649	6	0.28000	19	334
14	39.5790	2.27519	29	0.32690	93	1734
15	41.7940	2.15958	8	0.34800	25	538
16	43.6700	2.07106	5	0.26000	16	286
17	45.1466	2.00669	4	0.25330	12	194
18	46.4753	1.95237	30	0.30270	95	1653
19	47.8925	1.89785	12	0.36500	39	707
20	48.3700	1.88023	5	0.34000	17	301
21	49.2822	1.84754	30	0.29780	95	1430
22	50.2688	1.81357	20	0.28890	64	1023
23	51.0409	1.78793	15	0.26470	49	763
24	51.8600	1.76160	12	0.33340	38	657
25	53.0225	1.72568	13	0.32500	42	692
26	55.6716	1.64968	7	0.28330	22	370
27	56.9200	1.61643	4	0.24000	14	222
28	59.7125	1.54733	7	0.28500	22	336
29	60.2150	1.53561	4	0.31000	13	222
30	61.4300	1.50812	7	0.26000	22	377
31	62.7900	1.47869	10	0.26000	31	482
32	63.8875	1.45591	10	0.33500	31	544
33	64.8316	1.43697	9	0.31670	30	537
34	66.2066	1.41042	4	0.21330	13	190
35	71.4350	1.31948	4	0.39000	14	268
36	72.0400	1.30988	4	0.28000	13	218
37	73.7750	1.28331	5	0.35000	16	386

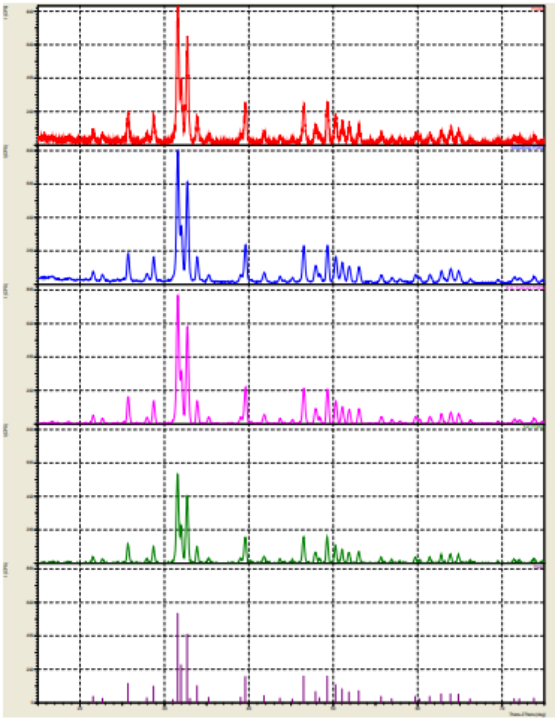

Sampel B

Strongest 3 peaks

no.	peak no.	2Theta (deg)	d (A)	I/I1	FWHM (deg)	Intensity (Counts)	Integrated Int (Counts)
1	7	31.8012	2.81163	100	0.71250	214	7465
2	8	32.8115	2.72733	71	0.56700	152	4515
3	16	46.6525	1.94537	29	0.49500	63	1610

Peak Data List

peak no.	2Theta (deg)	d (A)	I/I1	FWHM (deg)	Intensity (Counts)	Integrated Int (Counts)
1	21.6950	4.09308	5	0.47000	11	291
2	22.7950	3.89799	6	0.41000	12	267
3	25.2000	3.53117	3	0.20000	6	90
4	25.8200	3.44776	21	0.52000	46	1221
5	28.0400	3.17963	5	0.48000	10	244
6	28.8550	3.09165	18	0.51000	38	976
7	31.8012	2.81163	100	0.71250	214	7465
8	32.8115	2.72733	71	0.56700	152	4515
9	34.0100	2.63391	15	0.46000	33	773
10	35.3700	2.53569	5	0.38000	11	231
11	39.1400	2.29969	5	0.48000	11	291
12	39.7260	2.26711	29	0.50800	61	1611
13	41.9850	2.15020	7	0.55000	16	456
14	43.9200	2.05985	5	0.56000	10	275
15	45.3200	1.99942	3	0.36000	6	106
16	46.6525	1.94537	29	0.49500	63	1610
17	48.0950	1.89034	11	0.57000	24	747
18	49.4525	1.84158	27	0.47500	57	1355
19	50.4385	1.80786	18	0.45300	39	920
20	51.2166	1.78221	14	0.47330	30	730
21	52.0425	1.75585	11	0.46500	24	580
22	53.1866	1.72075	12	0.45330	25	630
23	55.8325	1.64531	7	0.46500	14	333
24	57.0900	1.61202	4	0.34000	9	171
25	60.0800	1.53874	8	0.88000	18	856
26	61.6000	1.50437	9	0.50000	19	487
27	63.0000	1.47426	11	0.54000	23	674
28	64.0450	1.45270	14	0.53000	31	839
29	65.0100	1.43345	13	0.50000	27	731
30	66.3900	1.40697	3	0.42000	7	208
31	69.5800	1.35005	4	0.32000	8	190
32	71.5800	1.31717	7	0.44000	15	357
33	72.2000	1.30737	4	0.36000	9	216
34	73.9100	1.28130	7	0.50000	14	393

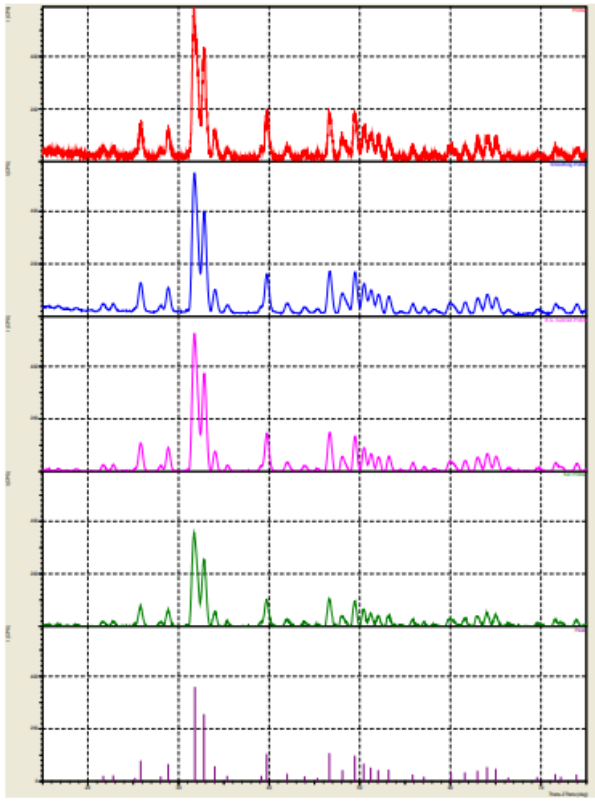

Sampel C

Strongest 3 peaks

no.	peak no.	2Theta (deg)	d (A)	I/I1	FWHM (deg)	Intensity (Counts)	Integrated Int (Counts)
1	6	31.7393	2.81697	100	0.29200	392	5818
2	8	32.8660	2.72293	74	0.28370	292	4536
3	7	32.1400	2.78276	46	0.33140	179	3025

Peak Data List

peak no.	2Theta (deg)	d (A)	I/I1	FWHM (deg)	Intensity (Counts)	Integrated Int (Counts)
1	21.7350	4.08564	6	0.29000	24	373
2	22.8525	3.88831	5	0.22500	18	222
3	25.8702	3.44119	22	0.25610	87	1285
4	28.1325	3.16939	7	0.22500	26	310
5	28.8920	3.08778	17	0.29600	67	1069
6	31.7393	2.81697	100	0.29200	392	5818
7	32.1400	2.78276	46	0.33140	179	3025
8	32.8660	2.72293	74	0.28370	292	4536
9	34.0450	2.63128	19	0.26500	76	1096
10	35.4275	2.53170	6	0.23500	23	300
11	39.1716	2.29791	6	0.27670	23	353
12	39.7588	2.26531	29	0.29580	114	1833
13	41.9850	2.15020	7	0.33000	27	556
14	43.8625	2.06242	5	0.20500	21	282
15	45.3333	1.99886	4	0.22670	17	221
16	46.6615	1.94501	31	0.29190	123	2007
17	48.0790	1.89093	13	0.30470	52	868
18	48.5616	1.87326	6	0.26330	22	299
19	49.4712	1.84092	32	0.27250	126	1838
20	50.4535	1.80736	19	0.28300	76	1196
21	51.2333	1.78167	13	0.30670	52	866
22	52.0606	1.75528	14	0.26530	54	756
23	53.2100	1.72005	14	0.26000	54	796
24	55.8213	1.64561	6	0.34930	24	439
25	57.1100	1.61150	4	0.34000	16	394
26	59.9150	1.54258	7	0.29000	28	467
27	60.3475	1.53256	4	0.26500	15	260
28	61.6200	1.50393	8	0.28000	31	542
29	62.9641	1.47502	9	0.26170	37	613
30	64.0520	1.45256	10	0.33600	40	689
31	64.9585	1.43447	10	0.26700	39	628
32	71.5550	1.31756	5	0.33000	20	376
33	72.2250	1.30698	4	0.37000	14	280
34	73.8350	1.28241	6	0.43000	22	617